JOURNAL OF CATALYSIS 157, 190–200 (1995)

Dehydro-oligomerization of Methane to Ethylene and Aromatics over Molybdenum/HZSM-5 Catalyst

Laiyuan Chen, Liwu Lin,[1] Zhusheng Xu, Xinsheng Li,[2] and Tao Zhang

Dalian Institute of Chemical Physics, Chinese Academy of Sciences, P.O. Box 110, Dalian 116023, People's Republic of China

Received August 31, 1994; revised April 6, 1995; accepted July 11, 1995

The structures of Mo/HZSM-5 catalysts with various molybdenum loadings were studied by means of XRD, IR, UV diffuse reflectance spectroscopy, TPR, and ammonia adsorption and desorption measurements. Both the BET surface areas and the acidities of catalysts decrease with an increase in molybdenum loading in the catalyst. The threshold of a monolayer dispersion of molybdenum is about 5 g of molybdenum per 100 g of HZSM-5 zeolite. Methane conversion under nonoxidizing conditions over Mo/HZSM-5 catalyst was tested. It was found that the catalyst with a molybdenum loading of 2–3 wt% exhibits optimum activity for the dehydro-oligomerization of methane to aromatics. Modifications of the 2% Mo/HZSM-5 catalyst with lithium or phosphorus cause a decrease in the acidity of the catalyst as well as in the catalyst activity. Addition of lithium shifts the selectivity toward ethylene at the expense of the yield of benzene. It is also demonstrated that the molybdenum oxide species are partially reduced by methane during the reaction. The removable lattice oxygen of molybdenum oxide oxidized adsorbed CH_x species to CO, which results in a side reaction to the catalytic oligomerization of methane to aromatics. The diminution of acidity of the catalyst and the blockage of the channels of HZSM-5 zeolite due to deposited carbon may be the main reasons for the deactivation of the catalyst. The methane oligomerization reaction is proposed to be catalyzed by molybdenum species located in the zeolite channels together with the Brønsted acid sites of HZSM-5 zeolite. A synergistic effect between these two kinds of centers plays an important role in the catalysis of the title reaction. Ethylene is identified to be a primary product while benzene is a final product in the dehydro-oligomerization reaction of methane. © 1995 Academic Press, Inc.

INTRODUCTION

The catalytic conversion of methane to desired chemicals or liquid fuel is still a challenging problem in the field of catalysis. Oxidative coupling of methane (OCM) is one of the most important research projects for the chemical utilization of methane during the past decade. Although significant progress has been achieved in the research and development of OCM (1), it is still difficult to overcome the barrier of technical–economic problems in connection with the low selectivity for C_2 hydrocarbons and the high heat of reaction released in this process. Therefore, recent attention has been paid to other pathways such as the partial oxidation of methane to synthesis gas, oxygenate compounds as well as hydrocarbons (2–4). The recent reports about the direct transformation of methane into aromatics open a new route for the exploration of novel catalytic processes. The initial studies of partial oxidation of methane over ZSM-5 zeolite by Shepelev and Ione (5–7) and Anderson and Tsai (8) demonstrated that the main products were CO, CO_2, and H_2O when oxygen was used as the oxidant. However, if N_2O was used, methane could be converted to aromatics selectively. Economically, it is more attractive to use air or oxygen as an oxidant instead of N_2O. Researchers at Exxon Research and Engineering Co. (9) have synthesized ethylene and benzene by alternatively switching methane and air over boron nitrides and carbide catalysts. By using a mixture of methane and oxygen ($CH_4:O_2:N_2 = 10:1:4$) as the reactants, Claridge *et al.* (10) have obtained a methane conversion of 13.2% and a hydrocarbon selectivity of greater than 48% at 1223 K over a $NaCl/MnO_2$ catalyst, operating at an elevated pressure (6 atm). More recently, Han *et al.* (11–13) reported the results of direct partial oxidation of methane with oxygen over HZSM-5 zerolite and metal-containing ZSM-5 catalysts; it was shown that higher hydrocarbons, in particular C_5^+ liquids, were produced.

Methane is very difficult to convert to higher hydrocarbons in the absence of any oxidant, due to its high stability (14). However, a number of authors have claimed that methane can be converted significantly under nonoxidative conditions in the presence of some appropriate catalysts. Bragin *et al.* (15) have realized the aromatization reaction of methane to benzene under nonoxidative conditions by pulse reaction over a $Pt\text{-}CrO_3/HZSM\text{-}5$ catalyst at 1023 K. A methane conversion of 18% with 14% yield of benzene was achieved. Wang *et al.* (16) also reported that a consid-

[1] To whom correspondence should be addressed.
[2] State Key Laboratory of Catalysis, DICP, CAS, China.

0021-9517/95 $12.00

erable conversion of methane to benzene with high selectivity could be obtained in a continuous reactor in the presence of a Mo/HZSM-5 catalyst. Over the MnO_x–Na/SiO_2–HZSM-5 catalysts and in the absence of any oxidant, methane can be transformed into aromatics with a yield similar to that reported for the oxidative coupling conditions (17). The aromatization of methane over amorphous-like carbon compounds has been briefly reported by Murata and Ushijima (18). Our recent work (19, 20) revealed that dehydro-oligomerization of methane to ethylene and benzene has taken place significantly under nonoxidizing conditions when a series of transition metal oxides incorporated with HZSM-5 were used as catalysts.

Thanks to the work cited above, the aromatization of methane has become a promising method for the catalytic transformation of methane. However, the problem is that the yield of aromatics is still rather low at present; more effective catalysts are needed. In addition, the mechanism of this reaction is still an open question. Therefore, in this paper, we report further the investigations on the conversion of methane over Mo/HZSM-5 catalysts with different molybdenum loadings. The modification of reaction performance by the addition of lithium and phosphorus and the influence of reaction temperature as well as the space velocity of methane were studied. The structures of these catalysts are characterized and a possible mechanism of methane transformation under nonoxidizing conditions over Mo/HZSM-5 catalyst is proposed.

EXPERIMENTAL

Preparation of Catalysts

The HZSM-5 zeolite with a SiO_2/Al_2O_3 ratio of 38 was obtained by four times repeated ion exchange of NaZSM-5 with an aqueous solution of ammonium nitrate (1 *N*) and was then calcined in air at 500°C for 6 h. The Mo/HZSM-5 catalysts were prepared by the impregnation method. A required amount of an aqueous solution of ammonium heptamolybdate (0.03 g Mo/ml, pH 6) was added to a beaker containing HZSM-5 powder; the slurry was agitated for 30 min at room temperature, then dried at 120°C for 10 h, and finally calcined in air at 720°C for 8 h. The color of the dried powder was light yellow, and it became darker with an increase in molybdenum content. However, all the samples turned white after calcination in air. The loading of molybdenum was 1, 2, 3, 5, 10, and 20 wt%, respectively.

Modifications of the 2% Mo/HZSM-5 catalyst by lithium and phosphorus were carried out by mixing the calcined 2% Mo/HZSM-5 catalyst with a nominal amount of lithium nitrate (0.05 *N*) or phosphoric acid (0.1 *N*) aqueous solution, and then dried and calcined under the same conditions as above.

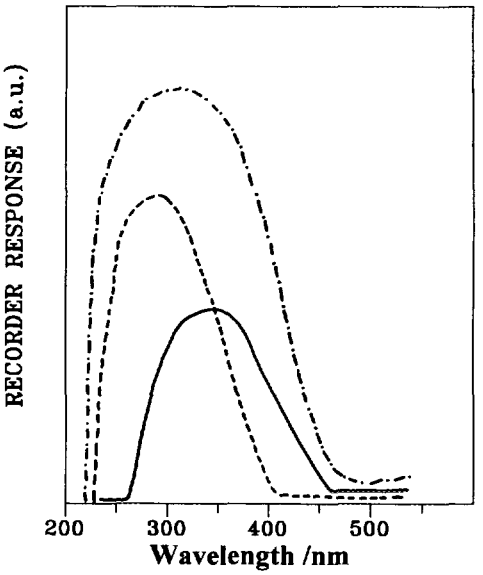

FIG. 1. UV diffuse reflectance spectra of (---) calcined 2% Mo/HZSM-5, (—) uncalcined 2% Mo/HZSM-5, and (-·-) pure MoO_3.

Characterization of Catalysts

BET surface areas and micropore volumes of the calcined catalysts were measured using a Micromeritics Instrument Corp. ASAP 2000 apparatus with nitrogen as the adsorbate. XRD measurements were performed with a Rigaku D/Max-rb 12 KW X-ray diffractometer operated at 50 KV and 40 mA with a scan speed of 8°/min from 5° to 60°. Infrared framework vibration spectra of the catalysts were obtained by using a Perkin–Elmer 580B infrared spectrometer with a resolution of 4 cm^{-1}. The sample was diluted with KBr in a ratio of 1:200(KBr), and then it was pressed into a self-supporting wafer for IR study. UV diffuse reflectance spectra (UV DRS) were recorded with

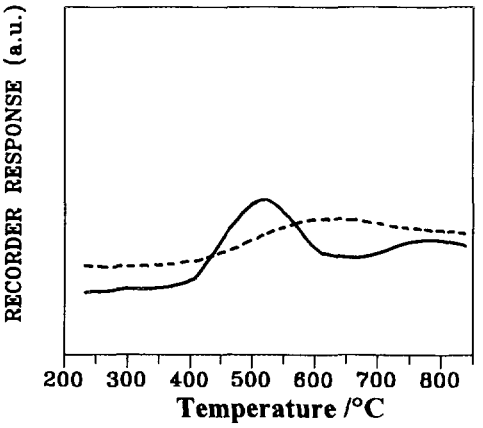

FIG. 2. TPR spectra of (---) calcined and (—) uncalcined 2% Mo/HZSM-5 catalysts.

TABLE 1

BET Surface Areas and Micropore Volumes of the Mo/HZSM-5 Catalysts with Different Molybdenum Loadings

Mo content (wt%)	BET surface areas (m^2/g)	Micropore volume (cc/g)
0	359.2	0.112
1	311.5	0.1098
2	319.9	0.1076
3	285.5	0.095
5	240.5	0.084
10	86.4	0.0376
20	76.2	0.034

a Hitachi MPF-4 fluorescence spectrophotometer. In these experiments, pure magnesium oxide was used as a reference. The scanning wavelength range was 200–500 nm and the scan speed was 120 nm/min. Temperature-programmed reduction (TPR) spectra were monitored in a conventional apparatus by using a 5% H_2/Ar mixture as reducing agent at a heating rate of 16°C/min. The acidity of catalysts was tested by measuring the ammonia uptake at 573 K after the catalyst was pretreated with helium at 973 K for 1 h, followed by a temperature-programmed desorption (TPD) of ammonia. The carbon deposition on the catalyst after reaction was studied by temperature-programmed oxidation (TPO), using a 10% O_2/He mixture as the oxidant. The CO_2 signal (m/e = 44) was monitored by an Anelva TS-360 quadrupole mass spectrometer.

The ESR spectra were recorded using a JES-FE2XG spectrometer operating at 9.5 GHz (X band). DPPH (g = 2.0036) was used for the determination of g values. The sample was loaded into a specially designed ESR tube, which provided the possibility for *in situ* treatment such as evacuation, reduction, and reaction. For the measurement of fresh catalyst, the sample-containing tube was evacuated by a mechanical pump for 1 h at 393 K to get a vacuum of about 1×10^{-2} Torr. The X-ray photoelectron spectra were obtained by using an Escalab MK-II spectrometer provided with a Mg anode X-ray exciting source (Mg$K\alpha$ 1253.6 eV, 9.6 KV, 30 mA). The pressure was maintained below 5×10^{-9} Torr during data acquisition. Calibration was made by charge referencing with the adventitious C_{1s} line at 284.6 eV.

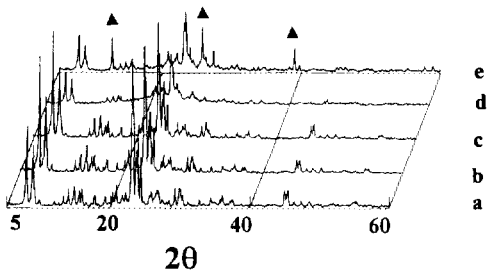

FIG. 3. XRD patterns of Mo/HZSM-5 catalysts with different molybdenum loadings: (a) HZSM-5, (b) 2% Mo/HZSM-5, (c) 5% Mo/HZSM-5, (d) 10% Mo/HZSM-5, and (e) 20% Mo/HZSM-5.

Catalytic Tests

Methane conversion tests were performed at atmospheric pressure in a quartz tubular flow microreactor (the dimensions of the reaction zone of the reactor were i.d. 8 mm, length 25 mm; other parts were filled with quartz) containing about 0.6 g of catalyst in each run. The catalyst was pretreated with flowing air at 973 K for 1 h, then in helium for half an hour to purge excess air, and finally a mixture of He and CH_4 was introduced into the reactor. The space velocity of methane was about 1400 ml/g cat · h and the flow rate ratio was CH_4:He = 1:1. The water in the products was removed by a drying agent before analysis of the products. An on-line gas chromatograph was used, equipped with Porapak QS columns, which were controlled in a temperature-programmed mode (from RT to 200°C), and a TC detector. The methane conversion and the product selectivity were calculated on a carbon number base.

The purity of methane was better than 99.95%; no hydrocarbon other than methane was detected in the analysis of this gas. The purity of helium was higher than 99.99%.

RESULTS AND DISCUSSION

Structure Characteristics of Mo/HZSM-5 Catalysts

BET surface areas of Mo/HZSM-5 catalysts with various molybdenum loadings are shown in Table 1. It can be seen that both the surface areas and the pore volumes decreased with increasing amounts of molybdenum. From this result we can visualize that the molybdenum species easily enter or block the channels of HZSM-5 zeolite and thus reduce the surface areas and the micropore volumes of the catalysts. When the molybdenum content increased from 10 to 20%, only a small decrease in the BET surface area as well as in the micropore volume of the catalyst was observed. This result implies that most of the channels of the HZSM-5 zeolite are blocked by molybdenum oxide species when its content approaches 10%; further increase in molybdenum content exhibited only a very small effect on the surface area.

In the preparation of the catalyst, the pH value of the impregnating solution was maintained at about 6; therefore, the predominant molybdenum species was heptamolybdate ions in the solution (21). During the impregnation stage, these species would be mainly adsorbed on the positive sites of the HZSM-5 zeolite as a result of the charge interaction. However, the chemical environment or the

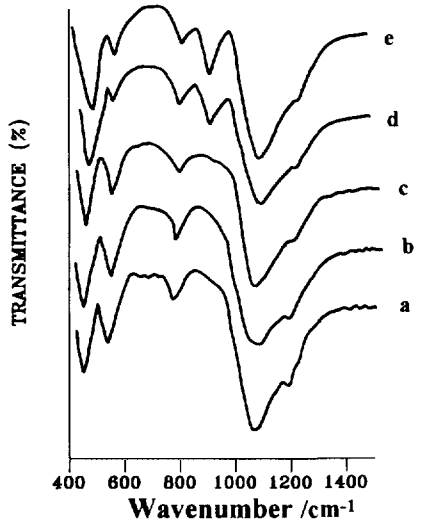

FIG. 4. Skeleton IR spectra of Mo/HZSM-5 catalysts with different molybdenum loadings: (a) HZSM-5, (b) 2% Mo/HZSM-5, (c) 5% Mo/HZSM-5, (d) 10% Mo/HZSM-5, and (e) 20% Mo/HZSM-5.

structure of molybdenum species changed significantly after high-temperature calcination of the catalyst. The UV diffuse reflectance spectra of an uncalcined 2% Mo/HZSM-5 sample and another which has been calcined at 993 K are compared in Fig. 1. The uncalcined sample exhibited its maximum absorption band at about 350 nm, which is referred to the characteristic adsorption band of heptamolybdate ions. It is interesting to note that this band shifted to about 300 nm after calcination. A possible explanation for this shift in the spectra is that the heptamolybdate ions decomposed into molybdenum trioxide after calcination at 993 K. An earlier report has shown that ammonium heptamolybdate was completely decomposed into molybdenum trioxide at a temperature lower than 973 K (22). The TPR profiles of the aforementioned samples are given in Fig. 2. It can be seen that the calcined 2% Mo/HZSM-5 catalyst was more difficult to reduce. The maximum reduction temperature of the calcined sample was about 873 K while for the uncalcined sample, two reduction peaks at about 773 and 1073 K were displayed. The difference in their reduction temperatures indicates that the heptamolybdate ions in the uncalcined sample behave as isolated species. After calcination, the molybdenum species are finely dispersed and interact strongly with the zeolite support, which may cause difficulty in the reduction of supported molybdenum oxide species in the calcined sample and prevent the sublimation of MoO_3. This result suggests that the predominant effect of calcination on the catalyst structure is the redispersion of the Mo species over the zeolite surface, which leads to the change in the chemical environment of molybdenum atoms, migration of Mo species into the channels of HZSM-5 zeolite, or a much stronger interaction of molybdenum species with the HZSM-5 zeolite (23, 24).

In addition to the dispersion of Mo, the catalyst structures and the molybdenum states also varied significantly with the change in the molybdenum loading of the catalyst. Phase analysis by XRD measurements demonstrated that only a HZSM-5 phase was observed when the molybdenum loading was low. Figure 3 suggests that the molybdenum species are finely dispersed on the surface or locate in the channels of the HZSM-5 zeolite when Mo content is less than 5% and no isolated molybdenum species can be detected in these samples. However, when the molybdenum loading exceeded 10%, crystals of molybdenum trioxide and polymolybdenum oxide species were present. Similar conclusions can also be drawn from the IR framework vibration spectra of these catalysts (shown in Fig. 4). The absorption band ascribed to the Mo–O–Mo vibration of polymolybdenum oxide at 917 cm^{-1} (22) could be observed only when the molybdenum loading exceeded 5%. The IR spectra of pure ammonium heptamolybdate and molybdenum trioxide were also recorded for comparison. Their absorption bands are as follows: ammonium heptamolybdate 921, 896, 843, 655, 581, and 474 cm^{-1}, and molybdenum trioxide 996, 869, 824, and 564 cm^{-1}. It is apparent that the 917 cm^{-1} band most probably resulted from the heptamolybdate species.

Figure 5 gives the UV diffuse reflectance spectra of Mo/HZSM-5 catalysts with different molybdenum loadings. According to Cacers (25), the range of the absorption band of tetrahedrally coordinated Mo(VI) is 200–300 nm, while that of octahedrally coordinated Mo(VI) is 260–400 nm.

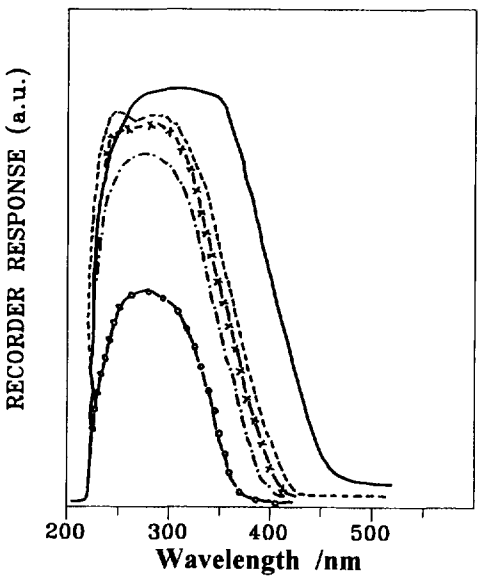

FIG. 5. UV diffuse reflectance spectra of (-O-) 1% Mo/HZSM-5, (-●-●) 2% Mo/HZSM-5, (-×-×) 5% Mo/HZSM-5, (---) 10% Mo/HZSM-5, and (—) pure MoO_3.

It can easily be seen in Fig. 5 that both concentrations of these two kinds of coordinated Mo(VI) ions increased with an increase in the molybdenum loading. However, the increment of the concentration of the tetrahedral species was more pronounced as compared to that of the octahedral species. When the Mo loading was greater than 5 wt%, the UV DRS spectra of different Mo/HZSM-5 catalysts hardly exhibited any difference. The XRD results show that the molybdenum trioxide phase appeared in the 20% Mo/HZSM-5 catalyst; however, the UV DRS spectrum and the IR spectrum of this catalyst were difficult from those of pure molybdenum trioxide. This probably implies that the molybdenum species supported on HZSM-5 is not in a free state as molybdenum trioxide; some other species perhaps exist. Furthermore, the interaction of these species with the support is possibly very significant.

It is speculated that during calcination, the molybdenum species can migrate from the surface of the HZSM-5 to its channels and disperse on the inner surface of the zeolite (26). As a result, the monolayer of the molybdenum species cannot be detected by XRD measurements, if the molybdenum loading is less than 5 wt%. It is also suggested from the XRD and IR spectra that the threshold of a monolayer dispersion is about 5 g molybdenum per 100 g of HZSM-5 zeolite. If the molybdenum loading is below this value, most of these species locate in the channels of the HZSM-5 zeolite. If it is above this value, an isolated molybdenum trioxide phase and polymolybdenum oxide species will appear as reported in the MoO_3/SiO_2 system (27). A highly dispersed species with terminal Mo=O sites appears at low molybdenum loading while polymolydenum species are formed at high molybdenum loading on the external surface of the catalyst.

Redox and Acid Properties of the Mo/HZSM-5 Catalysts

The TPR profiles of the Mo/HZSM-5 catalysts with different molybdenum contents are given in Fig. 6. We can see that the reduction peaks are small and flat when the molybdenum loading is lower than 5%. From earlier XRD and UV DRS studies, we knew that molybdenum species probably locate in the channels of the HZSM-5 and interact strongly with the zeolite when the molybdenum content is low. Therefore, the molybdenum oxide species are not easily reduced because of the strong oxide-support interaction. When the molybdenum loading increased to 5%, a noticeable reduction peak appeared at 823 K. This peak always appeared in the TPR profiles of all catalysts in which the molybdenum content was higher than 5% and the maximum reduction temperatures increased with an increase in molybdenum content. It is worth noting that the molybdenum oxide species can be reduced by hydrogen in the temperature range of 673–973 K, while the title reaction was also conducted in this temperature range.

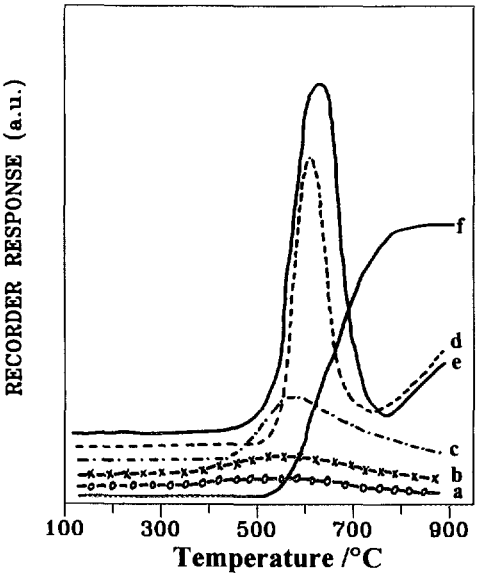

FIG. 6. TPR spectra of Mo/HZSM-5 catalysts with different molybdenum loadings. (a) 1% Mo/HZSM-5, (b) 2% Mo/HZSM-5, (c) 5% Mo/HZSM-5, (d) 10% Mo/HZSM-5, (e) 20% Mo/HZSM-5, and (f) pure MoO_3.

Therefore, the reduction of molybdenum oxide species probably occurs during the reaction.

The effect of molybdenum loading on the acidity of the Mo/HZSM-5 catalyst was studied by measuring the ammonia uptakes at 573 K. These data are listed in Table 2. Because the catalyst was pretreated with helium at 993 K before adsorption and the measurement was carried out at 573 K, the uptake of ammonia could be used to represent the number of strong acidic sites on the catalyst. Results in Table 2 show that with the introduction of molybdenum into the HZSM-5 zeolite, the number of acidic sites decreased, and the extent of the elimination of strong acid sites increased with an increase in molybdenum loading. Since ammonia may be decomposed into nitrogen and

TABLE 2

Ammonia Uptakes at 573 K on Mo/HZSM-5 Catalysts with Different Molybdenum Contents

Catalyst	NH_3 uptake (μ mol/g cat)
HZSM-5	241.1
1% Mo/HZSM-5	205.4
2% Mo/HZSM-5	169.6
3% Mo/HZSM-5	125.0
5% Mo/HZSM-5	102.7
10% Mo/HZSM-5[a]	75.9
20% Mo/HZSM-5[a]	53.6

[a] Ammonia uptakes at 473 K.

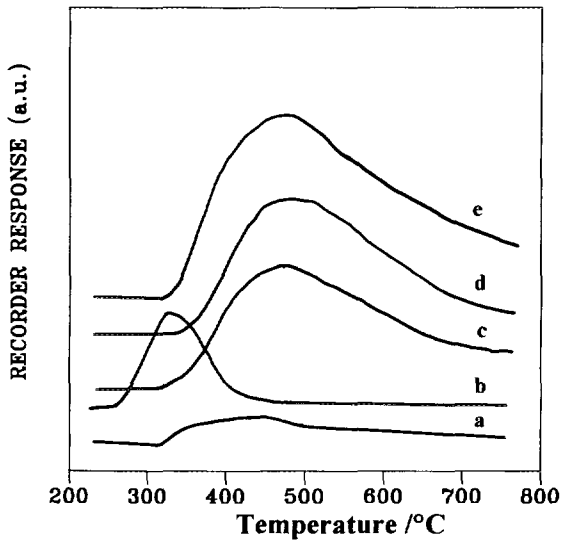

FIG. 7. Ammonia desorption profiles over Mo/HZSM-5 catalysts with different molybdenum loadings. (a) 20% Mo/HZSM-5, (b) 10% Mo/HZSM-5, (c) 5% Mo/HZSM-5, (d) 2% Mo/HZSM-5, and (e) 1% Mo/HZSM-5.

hydrogen at 573 K when the molybdenum loading exceeded 10%, the measurements of the ammonia uptakes of the 10 and 20% Mo/HZSM-5 catalysts were performed at 473 K. Figure 7 gives the NH_3 TPD spectra over the Mo/HZSM-5 catalysts with various molybdenum loadings. The maximum ammonia desorption temperatures decreased with increased molybdenum loading. For the 10% Mo/HZSM-5 and 20% Mo/HZSM-5 catalysts, ammonia desorbed at much lower temperatures. It is thus concluded that both the number and the strength of the acidic sites decrease with increased molybdenum loading in the HZSM-5 zeolite.

When the 2% Mo/HZSM-5 catalyst was modified by incorporating 0.1–1 wt% of lithium or phosphorus, the TPR spectrum as well as the IR spectrum did not change significantly. However, as we can see from Table 3, the addition of either modifier diminished the ammonia uptake of the catalyst. Ammonia desorption results also demonstrated that the maximum desorption temperature decreases as the lithium or phosphorus content increases. It is suggested that both lithium and phosphorus decrease the acidity of the 2% Mo/HZSM-5 catalyst.

TABLE 3

Effect of Lithium and Phosphorus Addition on Ammonia Adsorption at 573 K over a 2% Mo/HZSM-5 Catalyst

Modifier (wt%)	NH_3 uptakes (μ mol/g cat)
0	169.6
0.1% Li	151.8
1% Li	129.5
0.1% P	156.3
0.5% P	142.9
1% P	116.1

TABLE 4

Effect of Molybdenum Content on the Reaction Performances of Mo/HZSM-5 Catalysts

Mo content (wt%)	Methane conversion (%)	Selectivity (%)		
		CO	C_2H_4	C_6H_6
0	0.6	0.8	14.6	84.6
1	4.2	3.3	15.4	81.3
2	6.7	4.5	14.7	80.8
3	6.6	7.3	16.2	76.5
5	1.5	12.5	32.4	55.1
10	0.5	52.3	47.7	0
20	0.1	100	0	0

Note. There are significant amounts of water and hydrogen molecules in the products. Water was removed before analysis. The amount of H_2 was not quantified.

Catalytic Conversion of Methane

Table 4 gives the results of the dehydro-oligomerization of methane in the absence of any oxidant at 973 K over the Mo/HZSM-5 catalysts with different molybdenum contents. The unexpected catalytic activity of the zero Mo-loading HZSM-5 catalyst in producing ethylene and benzene, with the emergence of CO in the products in particular, defies conventional explanation. However, the oxygen in the product CO does give a clue to the origin of this catalytic activity. This oxygen could only come from the HZSM-5 zeolite. It has been concluded from the XPS studies on zeolites that the oxygen ions in the zeolitic system are subject to extensive polarization (28, 29). It has also been suggested that the oxygen ions in zeolites may be the catalytically active basic sites for certain reactions such as the dehydrogenation of isopropyl alcohol (30). It seems reasonable therefore to surmise that the enhanced electron density on the oxygen ions in HZSM-5 may initiate a nucleophilic attack on the incoming methane molecule at the reaction temperature for this zero Mo-loading system as the first step in forming the products experimentally observed.

It was found that the conversion of methane increases significantly after the introduction of molybdenum to the HZSM-5 zeolite; however, the optimum molybdenum content in the catalysts is about 2–3 wt% for the dehydro-oligomerization reaction of methane. Further addition of molybdenum results in a decrease in the activity and selec-

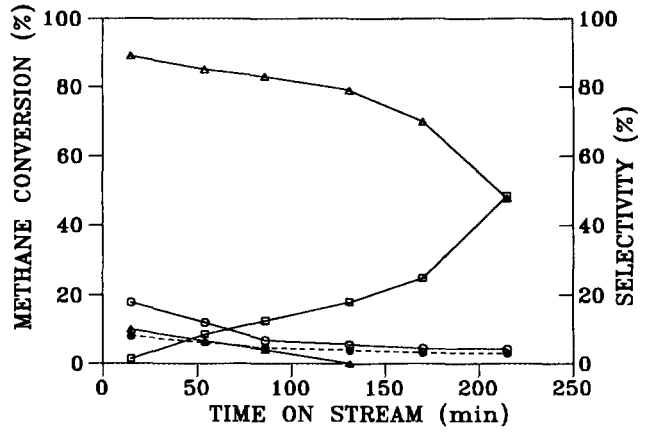

FIG. 8. Methane conversion and product selectivities as a function of methane time on stream over a 2% Mo/HZSM-5 catalyst. Catalyst pretreated with flowing air: (-○-) methane conversion, (-□-) selectivity for ethylene, (-△-) selectivity for benzene, (-▲-) selectivity of CO. Catalyst pretreated with flowing hydrogen: (-●-) methane conversion. T = 973 K, P = 1 atm, GHSV = 1400 ml/g cat · h.

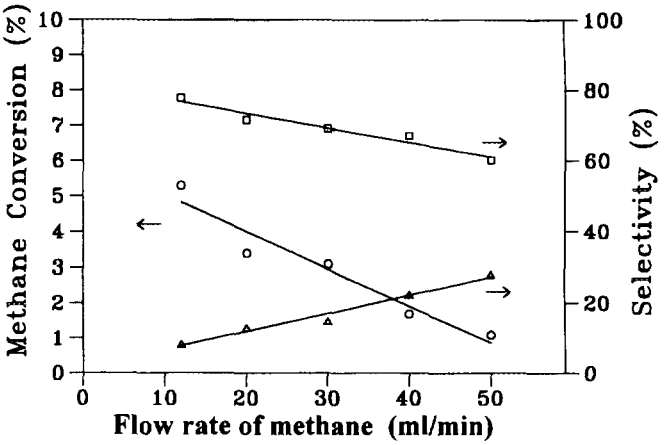

FIG. 9. Dependence of the reaction performances of a 2% Mo/HZSM-5 catalyst on the space velocity of methane. (-○-) methane conversion, (-△-) selectivity for ethylene, (-□-) selectivity for benzene. T = 973 K, P = 1 atm.

tivity of the catalyst for the conversion of methane to benzene. When the molybdenum content exceeded 5 wt%, the methane conversion was lower than 1% after methane was on stream for 1.5 h. It is obvious that with an increase in molybdenum loading, the selectivity for benzene decreased markedly. However, the selectivity for ethylene increased.

The methane conversion and product selectivities are given in Fig. 8 as a function of methane time on stream over a 2 wt% Mo/HZSM-5 catalyst. Methane conversion decreased considerably at the initial stage of the reaction, and then reached a constant level after methane was on stream for about 2 h. After the reaction was on stream for about 4 h, the catalyst was almost deactivated, and the conversion of methane was less than 1%. It is noteworthy that the selectivity of benzene decreased while the selectivity for ethylene increased with an increase in methane time on stream. This result demonstrates that ethylene is a primary product while benzene is a final product of the reaction. Possibly in the initial period of the reaction, carbon deposition was not very serious; that is, the Brønsted acid sites were not covered or blocked by the deposited carbon, and the primary product, ethylene, could easily aromatize into benzene. The rapid deactivation of the catalyst probably resulted from the deposited carbon, which could cover the acidic sites of the catalyst as well as block the channels of the zeolite.

The gas hourly space velocity of methane exerted significant influences on the reaction performance of methane conversion. Figure 9 reveals that with a decrease in the contact time of methane, the conversion of methane decreased substantially and the selectivity for ethylene increased while the selectivity for benzene decreased. This result substantiates the former suggestion that ethylene is a primary product while benzene is a final product in the title reaction. It is important to note from Fig. 9 that the total amount of converted methane, corresponding to the space time yield of total products, did not change significantly when space velocity varied in the range of 1400–6000 ml/g cat · h, although methane conversion decreased with an increase in methane space velocity. This result thus excludes the possibility of diffusion effects caused by the low flow rate (1400 ml/g cat · h) employed in our catalytic performance tests.

As expected from kinetic and thermodynamic considerations, high temperature will be advantageous to the title reaction. The influence of temperature on this reaction over a 2% Mo/HZSM-5 catalyst is shown in Fig. 10. It can be seen that this reaction initiated at about 873 K, but a

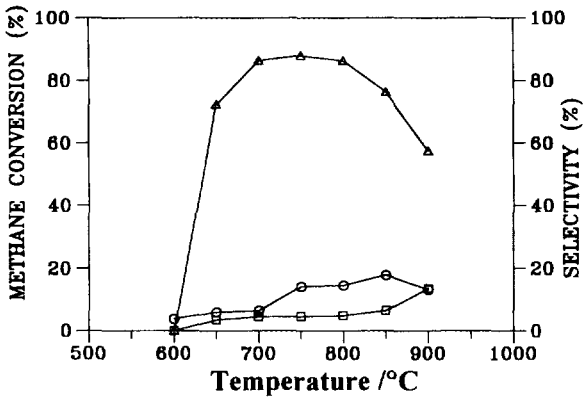

FIG. 10. Methane conversion and product selectivities as a function of reaction temperature over a 2% Mo/HZSM-5 catalyst. (-○-) methane conversion, (-□-) selectivity for ethylene, (-△-) selectivity for benzene. P = 1 atm, GHSV = 1400 ml/g cat · h.

TABLE 5

Effect of Modifiers on the Reaction Performances of a 2% Mo/HZSM-5 Catalyst

Modifier (wt%)	CH_4 conversion (%)	Selectivity (%)		
		CO	C_2H_4	C_6H_6
0.1% Li	4.2	11.2	23.1	65.7
0.5% Li	1.3	11.9	56.8	31.3
1% Li	0.3	44.8	55.2	0
0.1% P	5.4	11.5	8.7	79.8
0.5% P	4.6	15.9	8.4	75.7
1% P	3.4	16.5	10.5	73

Note. Data were taken after a methane time on stream of 1.5 h. Reaction conditions: T = 973 K, P = 1 atm, GHSV = 1400 ml/g cat · h

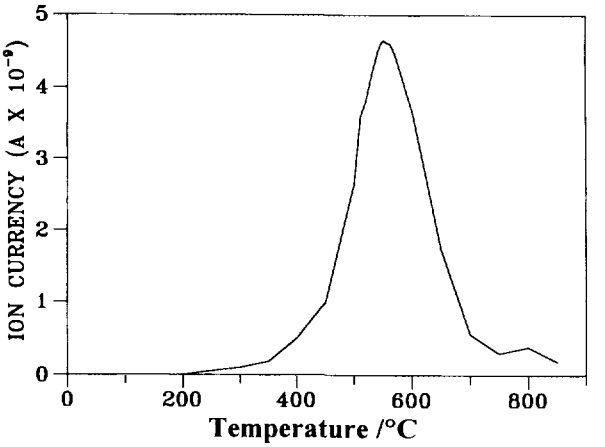

FIG. 11. TPO profiles of the deactivated 2% Mo/HZSM-5 catalyst. m/e = 44; the heating rate was 16 K/min.

significant methane conversion can be observed only when the temperature was over 923 K. However, if the temperature was too high, for example 1073 K, serious carbon deposition occurred, and therefore the conversion of methane and the selectivity for benzene decreased. It is thus suggested that the proper temperature range will be 973–1073 K for the aromatization of methane.

In an attempt to promote the 2% Mo/HZSM-5 catalyst, we tried to modify the catalyst by introducing lithium and phosphorus. The influences of these modifiers on methane conversion are given in Table 5. Unfortunately, both modifiers showed poisoning effects, which resulted in a decrease in catalyst activity, and the effect was more pronounced for lithium. When compared to the unmodified 2% Mo-ZSM-5 catalyst shown in Table 4, it can be seen that the addition of 0.1% Li reduced the methane conversion from 6.7 to 4.2%. However, the selectivity for ethylene increased from 14.6 to 23.1%. If the lithium content reached 1 wt%, the conversion of methane remained 0.3% while the selectivity for benzene decreased to zero. In this case, perhaps all the acidic sites were poisoned by lithium ions, which caused the loss of activity and the inhibition of the oligomerization of the intermediate ethylene to benzene. However, the high selectivity for ethylene provides the possibility for the development of nonoxidative coupling of methane to produce ethylene. The roles of promoters may be to slow down the rate of carbon deposition; therefore it is worthy to pay more attention to this aspect.

The Changes in the Nature of the Mo/HZSM-5 Catalyst after Deactivation

Serious carbon deposition on HZSM-5 zeolite during the reaction cannot be prevented at such a high temperature (973 K). The darkening of the catalyst after reaction was evidence of carbon formation. This kind of carbon, which was probably soot, could block the molybdenum surface and the channels of HZSM-5 zeolite, and thus impede the interaction of methane molecules with molybdenum species. It could also cover the acidic sites of the catalyst, and therefore, the catalyst would be completely deactivated eventually. Figure 11 gives the TPO spectrum of the deposited carbonaceous substances on the 2% Mo/HZSM-5 catalyst after methane reaction at 700°C for 1 h. We can see that only one peak of CO_2 appears in the TPO spectrum. This result implies that the deposited carbonaceous substance is homogeneous. DTA and TG results reveal that the amount of deposited carbon on catalysts increases in the following order: 20% Mo/HZSM-5 < 10% Mo/HZSM-5 < HZSM-5 < 5% Mo/HZSM-5 < 1-3% Mo/HZSM-5. Table 6 lists the ammonia uptakes over the reduced and deactivated 1% Mo/HZSM-5 catalysts. The uptake of ammonia by the catalyst decreased substantially after deactivation. Hydrogen reduction of the molybdenum species also resulted in a drop in the ammonia uptake, but the extent of the decrease was small as compared to that of the deactivated catalyst.

In order to investigate whether the valence state of molybdenum is changed after the deactivation of the 5% Mo/HZSM-5 catalyst, *in situ* TPR was carried out. It can be

TABLE 6

Ammonia Uptakes on Hydrogen Reduced and Deactivated 1% Mo/HZSM-5 Catalysts

Catalyst	NH_3 uptake (μ mol/g cat)
Deactivated[a]	147.3
H_2 reduced	178.6

[a] After methane was on stream for 4 h.

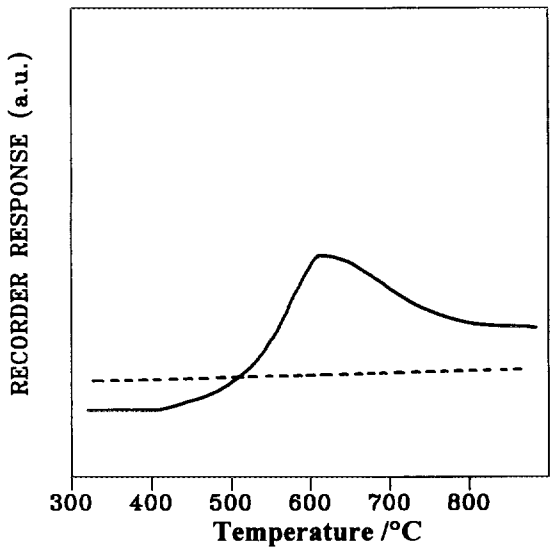

FIG. 12. TPR spectra of (—) fresh and (---) deactivated (after methane on stream for 4 h) 5% Mo/HZSM-5 catalysts.

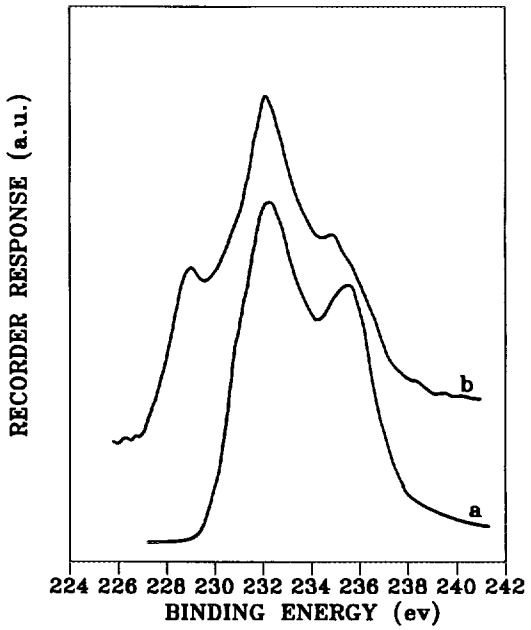

FIG. 14. XPS spectra of (a) fresh and (b) deactivated 2% Mo/HZSM-5 catalysts.

seen from Fig. 12 that the TPR profile of the deactivated catalyst was almost a straight line. By comparing it with the TPR profile of the fresh catalyst, it is clear that the states of the molybdenum species had changed and the active oxygen species was removed during the reaction. It is concluded that the molybdenum species are reduced by methane under reaction conditions. In order to further confirm this conclusion, *in situ* ESR experiments were performed. Figure 13 shows the ESR spectra of the 2% Mo/HZSM-5 catalyst subjected to different treatments. In the fresh catalyst, only a small Mo^{5+} signal was observed, which

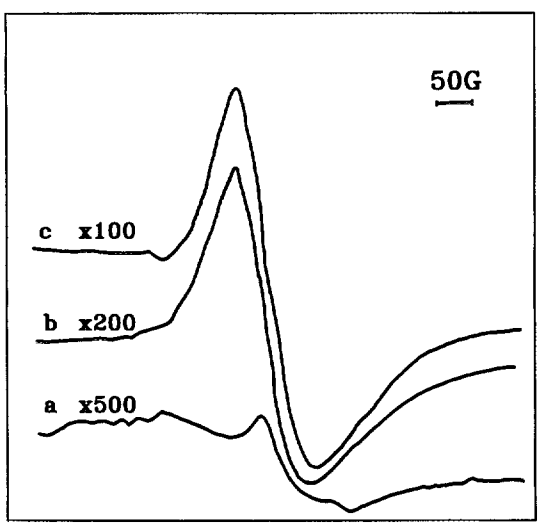

FIG. 13. ESR spectra of (a) fresh 2% Mo/HZSM-5 catalyst, (b) 2% Mo/HZSM-5 catalyst after flushing with methane at 873 K for 1 h, (c) 2% Mo/HZSM-5 catalyst after flushing with methane at 873 K for 2 h.

means that the oxidation state of Mo species was mainly +6. It is speculated from the $g_{\parallel}$ tensor that the Mo^{6+} was coordinated by oxygen (31). When this catalyst was heated at 600°C for 1 or 2 h under a flow of methane, the concentration of Mo^{5+} increased considerably, and the $g_{\parallel}$ value changed from 1.877 to 1.871. This observation led to the conclusion that the lattice oxygen of Mo-O species was removed during the reaction. This conclusion can be further substantiated by XPS results of the deactivated catalyst (Fig. 14). The binding energies of $Mo_{3d5/2}$ and $Mo_{3d3/2}$ were 232.5 and 235.5 eV, respectively, in the fresh catalyst. This result shows that the Mo^{6+} was predominant in this fresh catalyst. However, the Mo_{3d} bonding energies of 235.0, 232.1, and 229.0 eV were displayed in the deactivated catalyst. This clearly indicates the coexistence of Mo^{6+}, Mo^{5+}, and Mo^{4+} species in the spent catalyst (32, 33).

Carbon deposition on the catalyst is inevitable in this reaction and the Mo oxide species is reduced during the reaction. These two phenomena possibly exert a significant influence on the deactivation of the catalyst, and this kind of deactivation could be regenerated after burning off the carbon and reoxidizing the Mo species by oxygen treatment. Figure 15 shows the NH_3 TPD spectra of the fresh, reduced, and deactivated 1% Mo/HZSM-5 catalysts. We can see that the influence of reduction of the molybdenum species on the acidity of the catalyst was minor, while the ammonia uptake of the deactivated catalyst decreased remarkably. This implies that most of the acidic sites were lost during the reaction. The fact that the activity of catalyst could be revived after burning off the coke suggests that

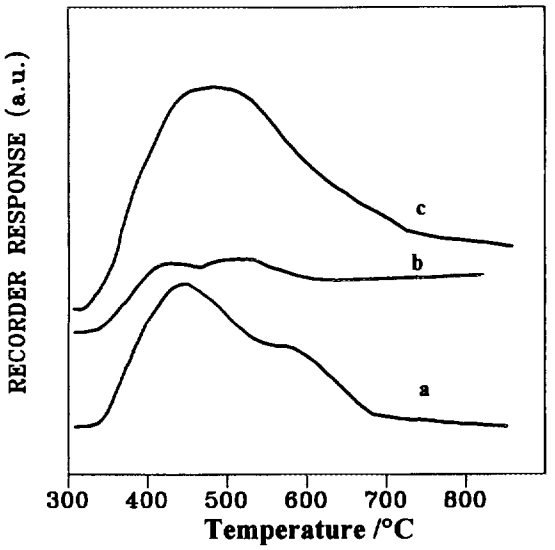

FIG. 15. Ammonia desorption spectra over (a) hydrogen reduced, (b) deactivated, and (c) fresh 1% Mo/HZSM-5 catalysts.

the significant loss of the acidic sites mainly results from the carbon deposition via the coverage of acidic sites or the blockage of the zeolite channels.

Possible Mechanism of Methane Conversion over Mo/HZSM-5 Catalyst

It can be seen from Table 4 that pure HZSM-5 zeolite showed some activity for this reaction. The occurrence of methane oligomerization over pure HZSM-5 possibly implies that the active oxygen ions as well as the Brønsted acidic sites on HZSM-5 zeolite are active centers for this reaction. In addition to the possible participation of the oxide ions and the Mo species in the HZSM-5 catalyst as mentioned earlier, the acidic sites may also take part in the activation of methane. In an earlier report on the oligomerization of methane without an oxidizing agent (34), the authors suggested that C–H bond cleavage can result from the protonation of fluorinated mordenite by superacid centers. As early as the 1960s, Olah reported that the activation of methane over superacid occurs via the formation of a CH_5^+ intermediate (35). However, the acidity of HZSM-5 is not strong enough to produce enormous amounts of CH_5^+; therefore, the methane conversion is rather low.

Pure molybdenum trioxide showed almost no activity for methane conversion. The introduction of molybdenum into HZSM-5 zeolite improved the conversion of methane significantly. However, if an excessive amount of molybdenum were added, methane conversion would decrease. XRD and IR results show that a molybdenum trioxide phase and polymolybdenum species would appear in the Mo/HZSM-5 catalyst in which the Mo content is higher than 10%. Therefore, it is suggested that molybdenum trioxide alone is not the active center for the conversion of methane, and also the polymolybdenum oxide species may deteriorate the activity for the formation of higher hydrocarbons. These results help us to conclude that the dispersion of the molybdenum species on HZSM-5 zeolite is crucial to the catalysis of the title reaction.

It is interesting to note that both the acidic sites and the molybdenum species are needed to catalyze the methane oligomerization significantly. It seems possible that the methane conversion was catalyzed by the molybdenum species inside the HZSM-5 channels together with the strong acidic sites of the HZSM-5 zeolite. The synergistic effect between these two kinds of sites plays a crucial role in the aromatization of methane. We tentatively propose the possible reaction schemes.

$$CH_4 \xrightarrow[H^+]{MoO_x} CH_3\cdot + H\cdot \qquad [1]$$

$$2CH_3\cdot \xrightarrow{MoO_x} C_2H_4 + H_2 \qquad [2]$$

$$3C_2H_4 \xrightarrow{H^+} C_6H_6 + 3H_2\cdot \qquad [3]$$

In the first step, the activation of methane to form $CH_3\cdot$ free radicals occurs via a concerted action between MoO_x and the Brønsted acidic sites. A misbalance of these two sites will impede the occurrence of this reaction. The $CH_3\cdot$ radicals can dimerize to form ethane and then ethylene easily. Finally ethylene aromatizes to benzene with the aid of the protons of HZSM-5 zeolite.

The activation of methane was catalyzed by a bifunctional catalyst in a manner somewhat similar to the aromatization of other higher hydrocarbons. However, as the activation of methane is rather difficult, a much higher temperature is required in order to acquire a desired conversion level. The high temperature employed in this reaction inevitably raises the problem of the reduction of molybdenum oxide in the catalyst. The fact that the molybdenum oxide was reduced by methane or adsorbed CH_x species during the reaction was substantiated by TPR, ESR, and XPS measurements. This reduction of molybdenum oxide is a side reaction, which results in the formation of by-product CO for the Mo-containing catalysts. However, this is a stoichiometric reaction. When the removable lattice oxygen was completely consumed, the production of CO ceased. This suggestion was supported by the fact that the amount of CO decreased drastically with methane time on stream, and dropped to zero after about 2 h on stream for a 2% Mo/HZSM-5 catalyst (Fig. 8). Over the catalyst which was reduced by hydrogen before the introduction of methane, no CO was detected in the products.

In addition, the conversion of methane is low, but this level was relatively constant during the reaction.

CONCLUSIONS

The main species of molybdenum is isolated heptamolybdate ions in the uncalcined Mo/HZSM-5 sample; however, the chemical environment of molybdenum in the catalyst is greatly altered after calcination in air. The structure of the Mo/HZSM-5 catalyst is quite different if the molybdenum content is different. A molybdenum content of 5% seems to be a threshold for a monolayer dispersion of molybdenum of HZSM-5 zeolite. Molybdenum species at this level probably locate in the channels of HZSM-5 in the Mo/HZSM-5 catalyst; they thus reduce the BET surface area and micropore volume, as well as the surface acidity of the catalyst. When above 5%, an isolated molybdenum trioxide phase and polymolybdenum oxide species will appear and decrease the surface area of the catalyst drastically.

The optimum molybdenum content of Mo/HZSM-5 catalyst is about 2–3% for the catalysis of the dehydro-oligomerization of methane. It is demonstrated that ethylene is a primary product and benzene is a final product in the reaction. The preferred temperature range for the production of benzene would be 973–1073 K. Modifications of the Mo/HZSM-5 catalyst with lithium and phosphorus result in a diminution of the conversion of methane; however, the selectivity for ethylene is enhanced considerably.

The synergistic effect between the well-dispersed molybdenum oxide species and the acidic sites of HZSM-5 is required for the catalysis of the dehydro-oligomerization of methane under nonoxidative conditions. The molybdenum species are reduced by methane during the reaction, which results in the formation of a small amount of CO at the initial stage of the reaction. The most probable reason for the deactivation of the catalyst is the serious carbon deposition on the catalyst, which blocks the channels and covers the acidic sites of the HZSM-5 catalyst. The deactivated catalyst can be regenerated by burning off the coke.

ACKNOWLEDGMENTS

The authors are grateful to Professor Hongli Wang for helpful discussions. The financial support for this work by the National Natural Sciences Foundation of China is greatly appreciated.

REFERENCES

1. Lunsford, J. H., *in* "New Frontiers in Catalysis," Studies in Surface Science and Catalysis, Vol. 75, Part A, p. 103. Elsevier, Amsterdam, 1993.
2. Chang, Y. F., and Heinemann, H., *Catal. Lett.* **21,** 215 (1993).
3. Matsumura, Y., and Moffat, J. B., *J. Catal.* **148,** 323 (1994).
4. Koranne, M. M., Goodwin, J. G., and Marcelin, G., *J. Catal.* **148,** 378 (1994); **148,** 388 (1994).
5. Shepelev, S. S., and Ione, K. G., *React. Kinet. Catal. Lett.* **23** (3/4), 319 (1983).
6. Shepelev, S. S., and Ione, K. G., *React. Kinet. Catal. Lett.* **23** (3/4), 323 (1983).
7. Shepelev S. S., and Ione, K. G., *J. Catal.* **117,** 362 (1989).
8. Anderson, J. R., and Tsai, P., *Appl. Catal.* **19,** 141 (1985).
9. Mitchell, H. L., and Wanghorne, R. H., U.S. Patent 4507517, U.S. Patent 4329658.
10. Claridge, J. B., Green, M. L. H., Tsang, S. C., and York, A. P. E., *Appl. Catal. A* **89,** 103 (1992).
11. Han, S., Martenak, D. J., Palermo, R. E., Pearson, J. A., and Walsh, D. E., *J. Catal.* **136,** 578 (1992).
12. Han, S., Martenak, D. J., Palermo, R. E., Pearson, J. A., and Walsh, D. E., *J. Catal.* **148,** 134 (1994).
13. Han, S., Martenak, D. J., Palermo, R. E., Pearson, J. A., and Walsh, D. E., *Catal. Lett.* **29,** 27 (1994).
14. Larkins, F. P., and Khan, A. Z., *Aust. J. Chem.* **42,** 1655 (1989).
15. Bragin, O. V., Vasina, T. V., Preobrazhenskii, A. V., and Minachev, K. M., *IZV Ser. Kim* **3,** 750 (1989).
16. Wang, L., Tao, L., Xie, M., Xu, G., Huang, J., and Xu, Y., *Catal. Lett.* **21,** 35 (1993).
17. Marczeuski, M., and Marczewska, K., *React. Kinet. Catal. Lett.* **53**(1), 33 (1994).
18. Murata, K., and Ushijima, H., *J. Chem. Soc. Chem. Commun.* **10,** 1157 (1994).
19. Chen, L. Y., Lin, L. W., Xu, Z. S., Zang, J. L., and Zhang, T., "Methane Activition Meeting, San Diego, CA, March 13–18, 1994." Preprints of Papers—American Chemical Society, Division of Petroleum Chemistry, Am. Chem. Soc., Washington, DC.
20. Chen, L. Y., Xu, Z. S., Zhang, T., and Lin, L. W., *Nat. Gas Chem. Ind.* (*CI Chem. Chem. Ind.*) (*Tianranqi Huagong*), **6,** 1 (1994).
21. Wang, L., and Hall W. K., *J. Catal.* **77,** 232 (1982).
22. Li, C., Xin, Q., Wang, K. L., and Guo, X. X., *Appl. Spectrosc.* **45**(5), 874 (1991).
23. Louis, C., and Che, M., *J. Catal.* **135,** 156 (1992).
24. Cid, R., Liambias, F. J., Fierro, J. L. G., Agudi, A. L., and Villasenor, J., *J. Catal.* **89,** 478 (1984).
25. Cacers, C. V., "Preparation of Catalysts III." p. 333. Elsevier, Amsterdam, 1983.
26. Thorect, J., Marchal, C., Doremieuxmorin, C., Man, P. P., Gruia, M., and Fraissard, J., *Zeolites* **13**(4), 269 (1993).
27. Smith, M. R., Zhang, L., Driscoll, S. A., and Ozkan, U. S., *Catal. Lett.* **19**(1), 1 (1993).
28. Barr, T. L., *Zeolites* **10,** 76 (1990).
29. Moretti, G., *Zeolites* **14,** 468 (1994).
30. Okamoto, Y., Ogawa, M., Maezawa, A., and Imanaka, T., *J. Catal.* **112,** 427 (1988).
31. Che, M., Bonneviot, L., Louis, C., and Kermarec, M., *Mater. Chem. Phys.* **13,** 201 (1985).
32. Holl, Y., Touroude, R., Maire, G., Muller, A., Engelhard, P. A., and Grosmangin, J., *J. Catal.* **104,** 202 (1987).
33. Grunert, W., Sakheev, A. Y., Morke, W., Feldhaus, R., Anders, K., Shpiro, E. S., and Minachev, K. M., *J. Catal.* **135,** 269 (1992).
34. Kowalak, S., and Moffat, J. B., *Appl. Catal.* **36,** 139 (1988).
35. Olah, G. A., and Schlossberg, R. H., *J. Am. Chem. Soc.* **90,** 2726 (1968).